

Primljen / Received: 4.4.2022.

Ispravljen / Corrected: 30.7.2022.

Prihvaćen / Accepted: 8.8.2022.

Dostupno online / Available online: 10.11.2022.

Effect of tightening zone length of reinforced concrete beams on beam capacity

Author:



Assist.Prof. **Sinan Cansız**, PhD. CE
Istanbul Arel University, Istanbul, Turkey
Faculty of Engineering
Department of Civil Engineering
sinancansiz@arel.edu.tr

Corresponding author

Research Paper

Sinan Cansız

Effect of tightening zone length of reinforced concrete beams on beam capacity

This study investigated seismic analysis of the behavior of reinforced concrete beams with various shear spans, stirrup shapes, and tightening zone lengths using the Seismostruct 2020 program. The load–displacement relations of 24 reinforced concrete beams with different conditions were modeled analytically. The analytical model used in the study was validated by comparing it with the experimental data from the literature. It was found that increasing the length of the tightening zone, particularly in beams with a high shear span, is essential for earthquake safety. In addition, the backbone curve of each beam was extracted, and comparison graphs were analyzed. The results obtained demonstrated that the length of the tightening zone limits the effect of stirrup shape and diameter on beam behavior.

Key words:

reinforced concrete beam, tightening zone, stirrup shape, seismic analysis

Prethodno priopćenje

Sinan Cansız

Utjecaj duljine kritičnog područja na nosivost armiranobetonskih greda

U ovom istraživanju provedena je seizmička analiza ponašanja armiranobetonskih greda s različitim posmičnim rasponima, oblicima spona i duljinama kritičnog područja pomoću programa SeismoStruct 2020. Odnosi između opterećenja i pomaka 24 armiranobetonske grede u različitim uvjetima analitički su modelirani. Analitički model korišten u istraživanju potvrđen je usporedbom s eksperimentalnim podacima iz literature. Utvrđeno je da je povećanje kritičnog područja, posebice kod greda s velikim posmičnim rasponom, važno za protupotresnu sigurnost. Nadalje, izdvojena je krivulja kapaciteta nosivosti svake grede i analizirani su usporedni grafikoni. Dobiveni rezultati pokazali su da duljina kritičnog područja ograničava učinak oblika i promjera spona na ponašanje grede.

Ključne riječi:

armiranobetonska greda, kritično područje, oblik spona, seizmička analiza

1. Introduction

Currently, reinforced concrete (RC) structures are the most widely employed structural system. After every earthquake occurrence, new design strategies for RC structures have been implemented. Especially, since the 1995 Kobe earthquake, there have been significant modifications to the design of RC structures. After earthquakes, structures designed with force-based approaches become unusable. As a result, new approaches need to be developed. These new design principles, emerging from strain-based approaches, dictates that RC elements be created with a particular performance objective [1-4].

Beams are a fundamental element of the reinforced concrete structural system and thus have been investigated by numerous researchers considering new design approaches. The experimental studies are limited in terms of cost and time. In some of these studies, the shear capacity of reinforced concrete beams was analyzed, and models based on shear span were developed. Many researchers have conducted studies on the shear span, the most important parameter that determines the fracture shape of beams, and as a result, seismic code recommendations have been made [5, 6].

Stirrups are the most important factor in determining the shear resistance of beams. Numerous researchers investigating the effect of stirrups on behavior have proposed various seismic code modifications [7-11]. Lateral reinforcement layouts for reinforced concrete elements are defined in seismic codes widely used worldwide. Stirrups are tightened to reduce damage in plastic hinge areas where intense damage is expected during earthquake loads. All seismic codes recommend taking various precautions in the plastic hinge areas where intense damage to beams is observed under earthquake loads. As the length of the plastic hinge region is typically expressed in terms of the section height, researchers have explained this value in terms of various parameters. Recent studies have revealed that the shear span influences the length of the plastic hinge [12, 13]. As seismic codes limit the plastic hinge region from exceeding two times the section height, the length of the stirrup tightening region is maintained at two times the section height. Considering the improvement in concrete quality and the advantages of concrete additives, many structures employ beams with extensive spans. In addition, the preference for short spans in conventional reinforced concrete structures has necessitated a re-evaluation of high-span beams.

In recent years, computer programs [14-16] have enabled the analytical modeling of numerous experimental sets with various parameters. In some studies, analytical models of experimental sets are created, and the results are compared. According to the results of the analysis, analytical models accurately predicted the experimental outcomes. Thus, investigating the effect of stirrup tightening zone lengths on reinforced concrete beams with varying shear spans using analytical models and validating them with experimental models will significantly contribute to

the literature. In this study, the seismic analysis of beams with different shear spans, stirrup conditions, and tightening zone lengths has been performed using the Seismo-Struct 2020 program. This study investigates the effect of the tightening zone length on the behavior of reinforced concrete beams and determines the optimal length of the tightening zone.

2. Materials and methods

Figure 1 depicts the stirrup tightening zone (hugging zone) in reinforced concrete beams, according to EUROCODE [17].

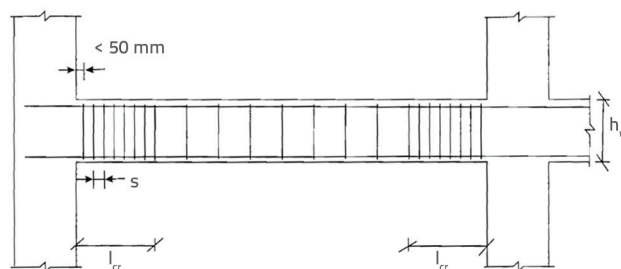


Figure 1. Transverse reinforcement in critical regions of beams for EUROCODE

From Fig. 1, the critical region is defined as l_{cr} equal to $2h$. Similarly, the Turkey earthquake building code (TBEC-2018) accepts $2h$ as the length of the critical section [18].

This study analyzed 24 reinforced concrete beams with various shear spans and stirrup conditions analytically, with load-displacement relations extracted using the Seismo-Struct program. The performance of RC beams using the material strain values in TBEC-2018 are determined. Panagiotakos and Fardis [19] proposed formulations for chord rotation capacity at yielding and "ultimate" (at 20% strength drop) strengths. The "ultimate" strength value was determined through an empirical and a semi-empirical (i.e., based on the plastic hinge length) approach derived from a large database of flexure-controlled experimental tests for RC elements.

According to TBEC-2018, the performance levels are calculated using material strain values. These calculations are depicted in equations (1)-(3).

$$\epsilon_c^{(CP)} = 0.0035 + 0.07\sqrt{\omega_{wc}} \leq 0.01 \tag{1}$$

$$\epsilon_s^{(CP)} = 0.04\epsilon_{su} \tag{2}$$

$$\theta_p^{(CP)} = \frac{2}{3} \left[(\phi_u - \phi_y) L_p \left(1 - 0.5 \frac{L_p}{L_s} \right) + 4.5\phi_u d_b \right] \tag{3}$$

where ϵ_c is the shortening in the outermost concrete compression fiber, ω_{wc} is the mechanical index of the lateral reinforcement, ϵ_s is the unit elongation of the longitudinal reinforcement, ϵ_{su} is the unit elongation at the moment of

maximum stress of the longitudinal reinforcement, θ_p is the plastic rotation of the element, ϕ_u is the maximum curvature of the section, ϕ_y is the yielding curvature of the section, L_p is the plastic joint length, L_s is the shear span, and d_b is the longitudinal reinforcement diameter.

EUROCODE-8 contains a section for assessing reinforced concrete beams, where it recommends estimating chord rotations using the given formulation in the code. This formulation is dependent on several variables, including the axial load ratio, longitudinal reinforcement ratio, transverse reinforcement ratio, and yield strength of the transverse reinforcement, as shown in Eq. (4).

$$\theta_{um} = \frac{1}{\gamma_{el}} 0.016 \times 0.3^{\rho} \left(\frac{\max(0.01w')}{\max(0.01w)} f_c \right)^{0.225} \left(\min\left(9; \frac{L_s}{h}\right) \right)^{0.35} 25^{\left(\frac{\rho_{sv}}{f_c}\right)} (1.25^{100\rho_d}) \quad (4)$$

where γ_{el} is the seismic element coefficient (equal to primary element is 1.5 and secondary element is 1), ρ is the dimensionless axial load levels ($N/A_c f_c$), h is the height of the section, w is the mechanical reinforcement ratio for compression and tension, L_s is the shear span, f_c is the concrete strength, f_{yv} is the transverse steel yield strength, ρ_{sv} is the ratio of transverse steel to parallel to the direction x of loading, α is the confinement effectiveness factor, and ρ_d is the steel ratio of diagonal reinforcement.

FEMA 356, the American code for the seismic rehabilitation of buildings, expresses the displacement limits of RC beams in the form of plastic rotations [20]. The following equations were used to estimate the plastic capacity for the limit state that prevents collapse.

$$\frac{\rho - \rho'}{\rho_{bal.}} \leq 0 \rightarrow \frac{V}{b_w d \sqrt{f_c}} \leq 3 \rightarrow \theta_{pl} = 0.025 \quad (5)$$

$$\frac{\rho - \rho'}{\rho_{bal.}} \leq 0 \rightarrow \frac{V}{b_w d \sqrt{f_c}} \leq 6 \rightarrow \theta_{pl} = 0.020 \quad (6)$$

$$\frac{\rho - \rho'}{\rho_{bal.}} \leq 0.5 \rightarrow \frac{V}{b_w d \sqrt{f_c}} \leq 3 \rightarrow \theta_{pl} = 0.020 \quad (7)$$

$$\frac{\rho - \rho'}{\rho_{bal.}} \leq 0.5 \rightarrow \frac{V}{b_w d \sqrt{f_c}} \leq 6 \rightarrow \theta_{pl} = 0.015 \quad (8)$$

3. Confirmation of the analytical model

The Seismo-Struct 2020 program was utilized to investigate the analytical results of RC beams [21]. The accepted material models for TBEC-2018 were selected and modeled in the program. In addition, the results of the experiments used in the literature are compared with the program's outputs to ensure that they are accurate. Two beam samples tested in the literature are modeled in the Seismo-Struct 2020 program. The comparison of the experimental data with the analytical data is shown in Figures 2 and 3.

When the correct material models were selected, the analytical results obtained were closest to the experimental data. Examining Figures 2 and 3 reveals that the analytical models closely predict the behavior of the experimental models. In the same model, modifying the length of the tightening zone and the shear span was also considered to achieve more uniform results.

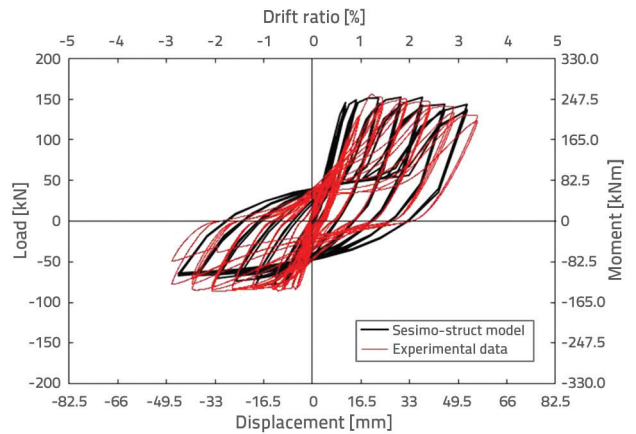


Figure 2. Comparison of experimental and Seismo-struct model data for K3.6YP1 specimen

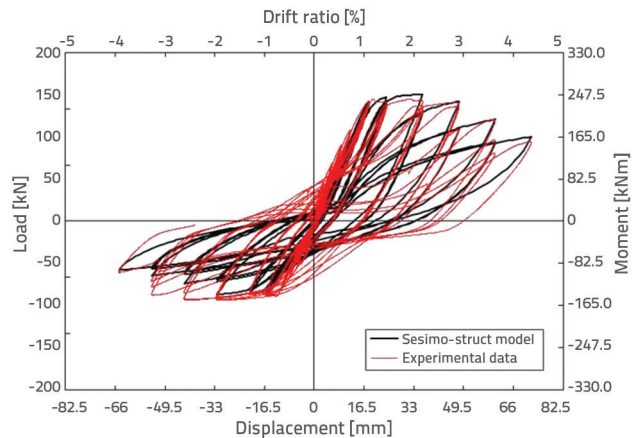


Figure 3. Comparison of experimental and Seismo-struct model data for K6.0YP1 specimen

3.1. Beam properties

The properties of the 24 RC beams examined in this article are presented in Table 1. From Table 1, a/d is the shear span to depth ratio and ϕ_s is the diameter of the stirrup. Within the scope of this study, the same reinforcement configuration was utilized for all models. For the longitudinal reinforcements, $4\phi 16$ is selected for both the upper and lower reinforcements. For the transverse reinforcements, 75 mm stirrup spacing in the tightening zone and 150 mm stirrup spacing in the beam spans were selected. The beam tightening zone lengths to be examined within the scope of the study are h - $2h$ - $3h$. Figure 4 depicts the cross-section of the beams modeled in the Seismo-Struct 2020 program, along with the schematic loading pattern and cross-section.

Table 1. Properties of the beams

Beam	a/d	ϕ_s	S	Tightening zone	Shape of stirrup
B-4-8-2-1H	4	8	Ø8/7.5/15	h	2
B-4-8-2-2H	4	8	Ø8/7.5/15	2h	2
B-4-8-2-3H	4	8	Ø8/7.5/15	3h	2
B-4-8-3-1H	4	8	Ø8/7.5/15	h	3
B-4-8-3-2H	4	8	Ø8/7.5/15	2h	3
B-4-8-3-3H	4	8	Ø8/7.5/15	3h	3
B-4-10-2-1H	4	10	Ø10/7.5/15	h	2
B-4-10-2-2H	4	10	Ø10/7.5/15	2h	2
B-4-10-2-3H	4	10	Ø10/7.5/15	3h	2
B-4-10-3-1H	4	10	Ø10/7.5/15	h	3
B-4-10-3-2H	4	10	Ø10/7.5/15	2h	3
B-4-10-3-3H	4	10	Ø10/7.5/15	3h	3
B-8-8-2-1H	8	8	Ø8/7.5/15	h	2
B-8-8-2-2H	8	8	Ø8/7.5/15	2h	2
B-8-8-2-3H	8	8	Ø8/7.5/15	3h	2
B-8-8-3-1H	8	8	Ø8/7.5/15	h	3
B-8-8-3-2H	8	8	Ø8/7.5/15	2h	3
B-8-8-3-3H	8	8	Ø8/7.5/15	3h	3
B-8-10-2-1H	8	10	Ø10/7.5/15	h	2
B-8-10-2-2H	8	10	Ø10/7.5/15	2h	2
B-8-10-2-3H	8	10	Ø10/7.5/15	3h	2
B-8-10-3-1H	8	10	Ø10/7.5/15	h	3
B-8-10-3-2H	8	10	Ø10/7.5/15	2h	3
B-8-10-3-3H	8	10	Ø10/7.5/15	3h	3

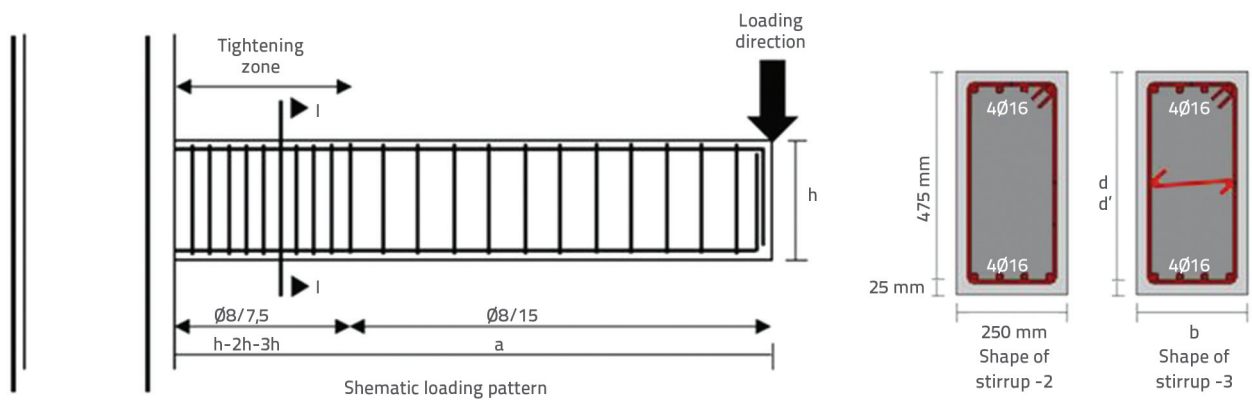


Figure 4. Schematic loading layout and section of the beams

3.2. Loading profile

All examined beams utilized an identical loading profile. Similar to the previous study by Lehmann and Moehle [23], increasing the amplitude of cyclic loading was applied from the beam end.

In this context, the analytically defined loading profile is shown in Figure 5.

Kunnath *et al.* examined the effect of loading profiles on the behavior of the reinforced concrete element [24]. They determined that the increasing cyclic loading more accurately reflects the

damage status of the RC element. In addition, when a large amount of experimental data from the literature were analyzed, it was discovered that increasing cyclic loads were utilized.

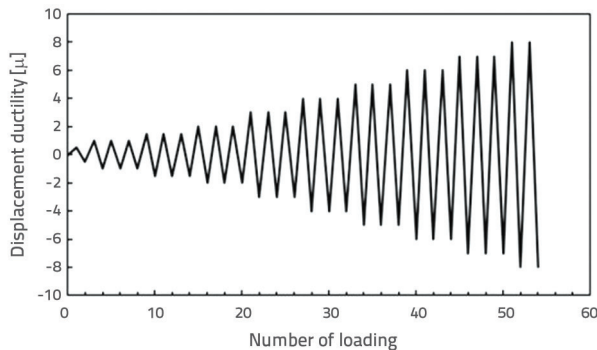


Figure 5. Schematic loading profile

While calculating the loading profile, a multiple of the yield displacement determined under monotonic loading was used. The displacement value, applied as half of the yield displacement before yielding, was applied once. It is defined as triple repetitive and increasing ductility multiples (1μ-1.5μ-2μ-3μ-4μ...) together with the yield displacement value.

3.3. Modeling in Seismo-Struct

The selection of material models is one of the key parameters affecting the behavior of the RC beam. The Managetto–Pinto model was used to describe the behavior of the reinforcement [25]. For the behavior of concrete, the model representing the nonlinear behavior defined by Mander *et al.* was used [26]. Images of the models defined in the program are shown in Figure 6.

In the validation models produced for comparison with the experimental results, the A1 parameter was set to 19.55. The

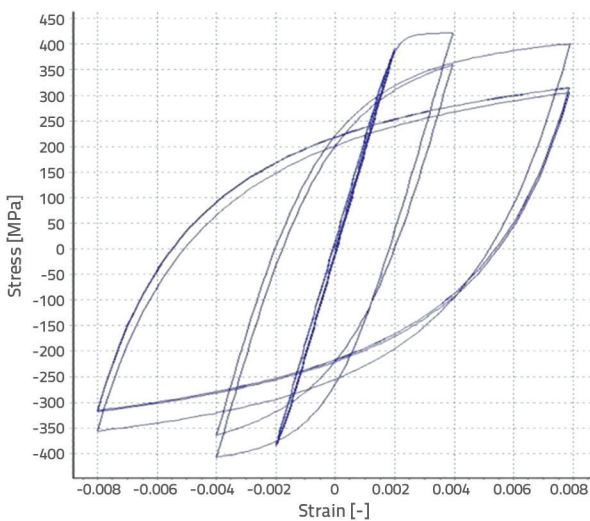


Figure 6a. Managetto-Pinto steel model

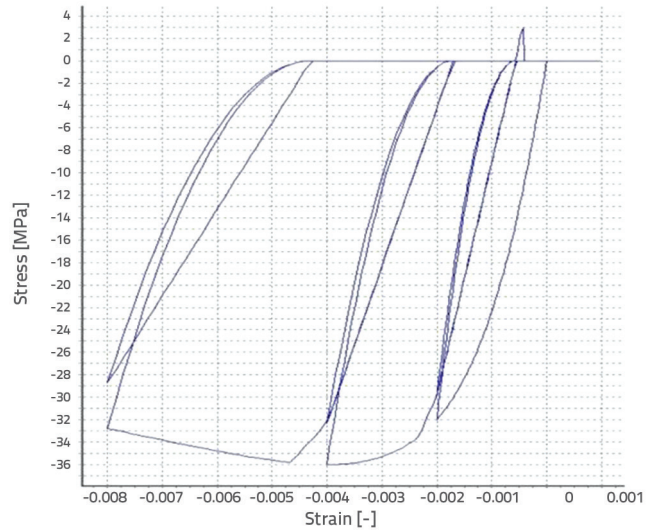


Figure 6b. Mander et al. concrete model

same value was used in all beam models to reduce the strength of the Managetto–Pinto model close to the real behavior. The tightening zone and the beam span region, which influence the beam behavior, are defined as separate sections and is designed with 75 mm spacing between the stirrups in the tightening zone and 150 mm spacing between the stirrups in the beam span. As these two beam regions are defined as two different sections in the program, the verification beams also consider these design factors. Keeping the stirrup spacing constant was shown to reflect the behavior correctly. Thus, the analytical model reflects the effect of the tightening zone as reflected by two different models. The view of the beam modeled in the program is shown in Figure 7.

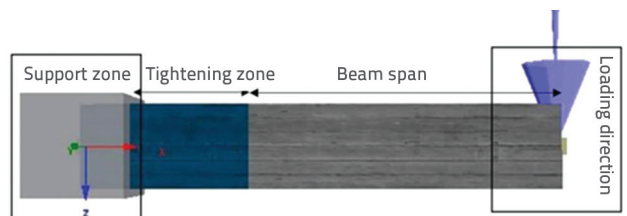


Figure 7. Screenshot of the model made in the Seismo-struct 2020 program

4. Analytical results

Figure 8 depicts the analytical results of a seismic analysis conducted under increased amplitude cyclic loading simulated from earthquake loads. Considering the load–displacement curves of the beams, the performance levels calculated according to TBEC-2018, FEMA356, and EUROCODE were calculated with the aid of 1–8 relations and marked. In addition, the displacement demand corresponding to a 20% reduction in lateral load carrying capacity is plotted on the curve for control purposes.

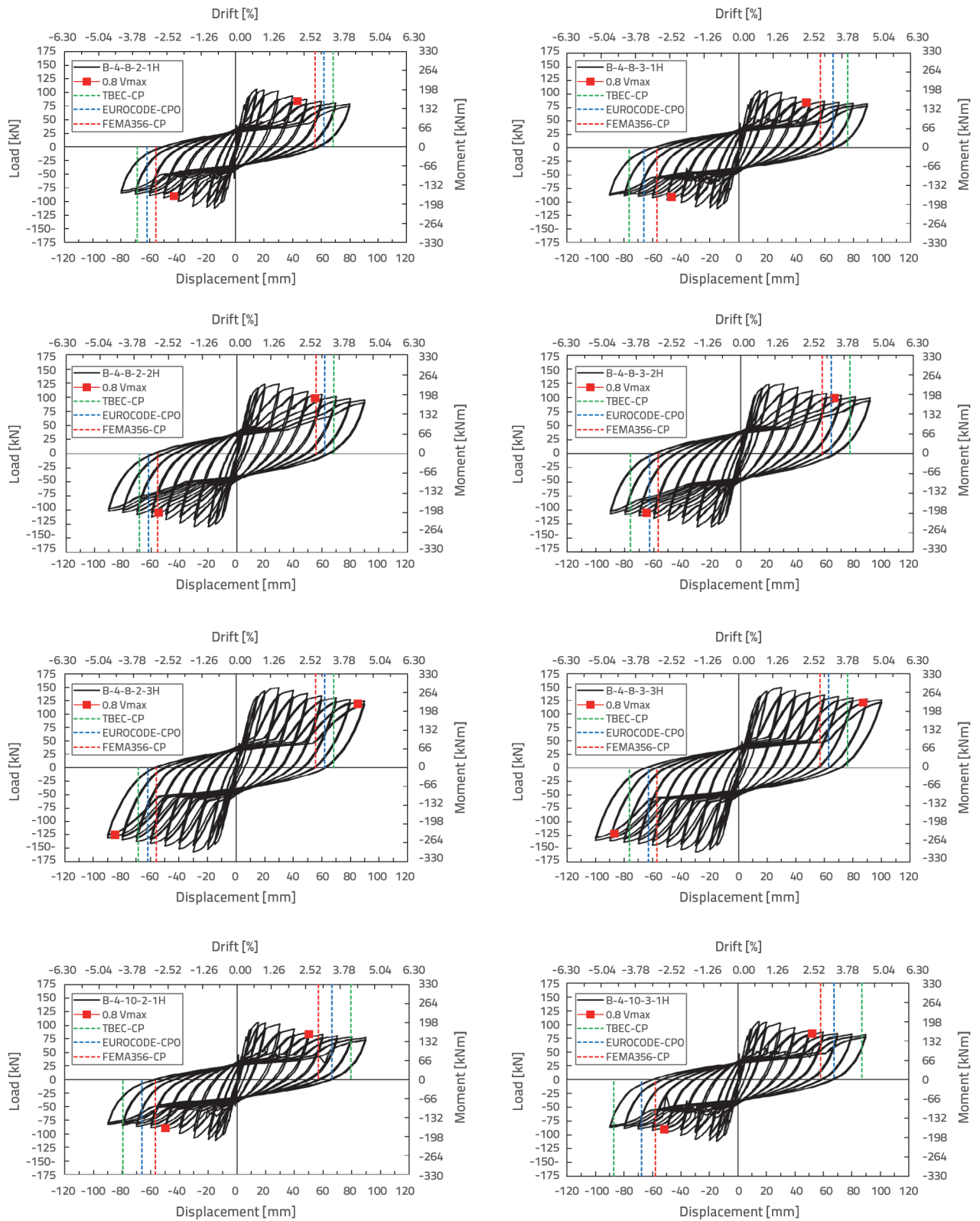


Figure 8. Load–displacement relationships of the beams

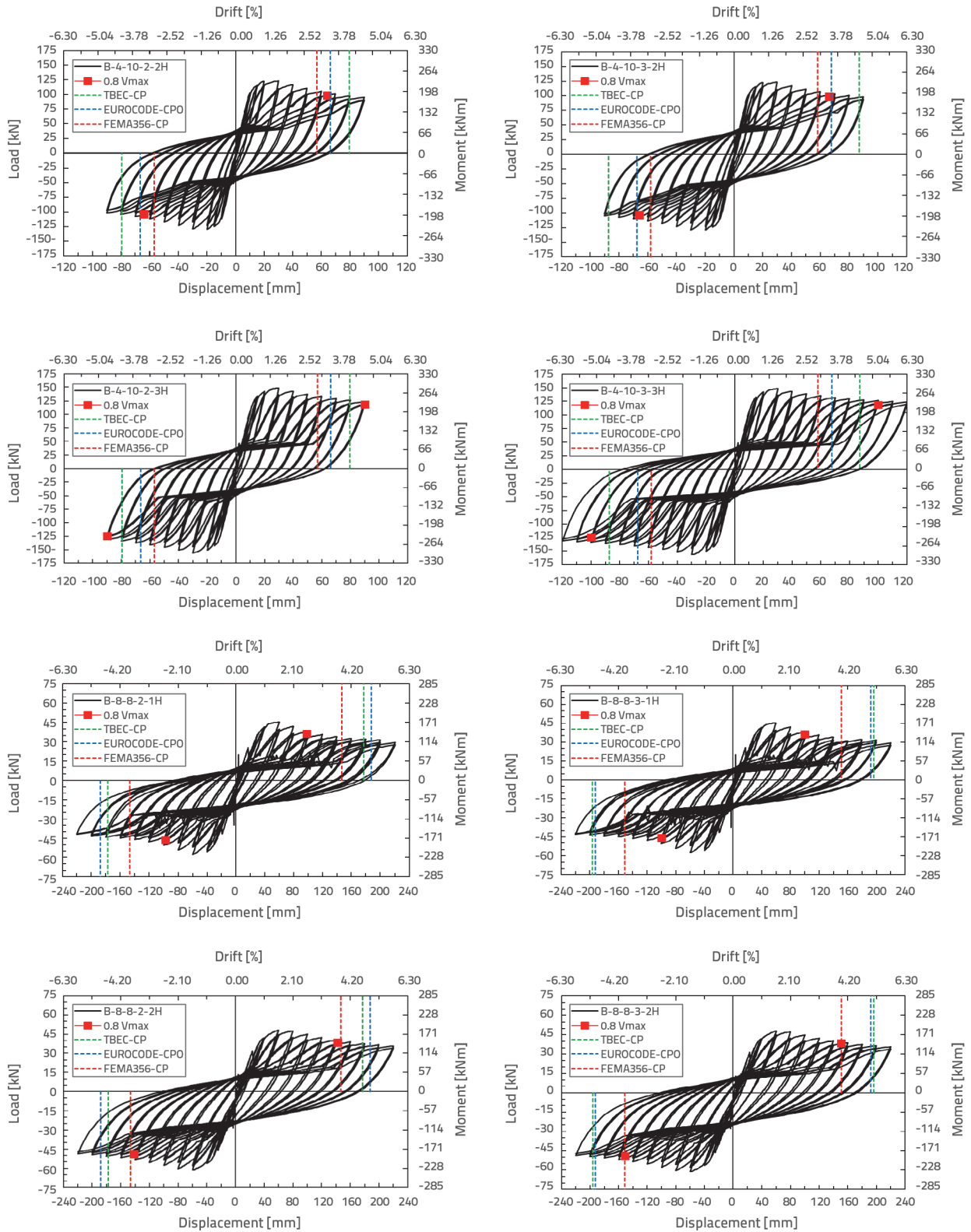


Figure 8. Load–displacement relationships of the beams - continuation 1

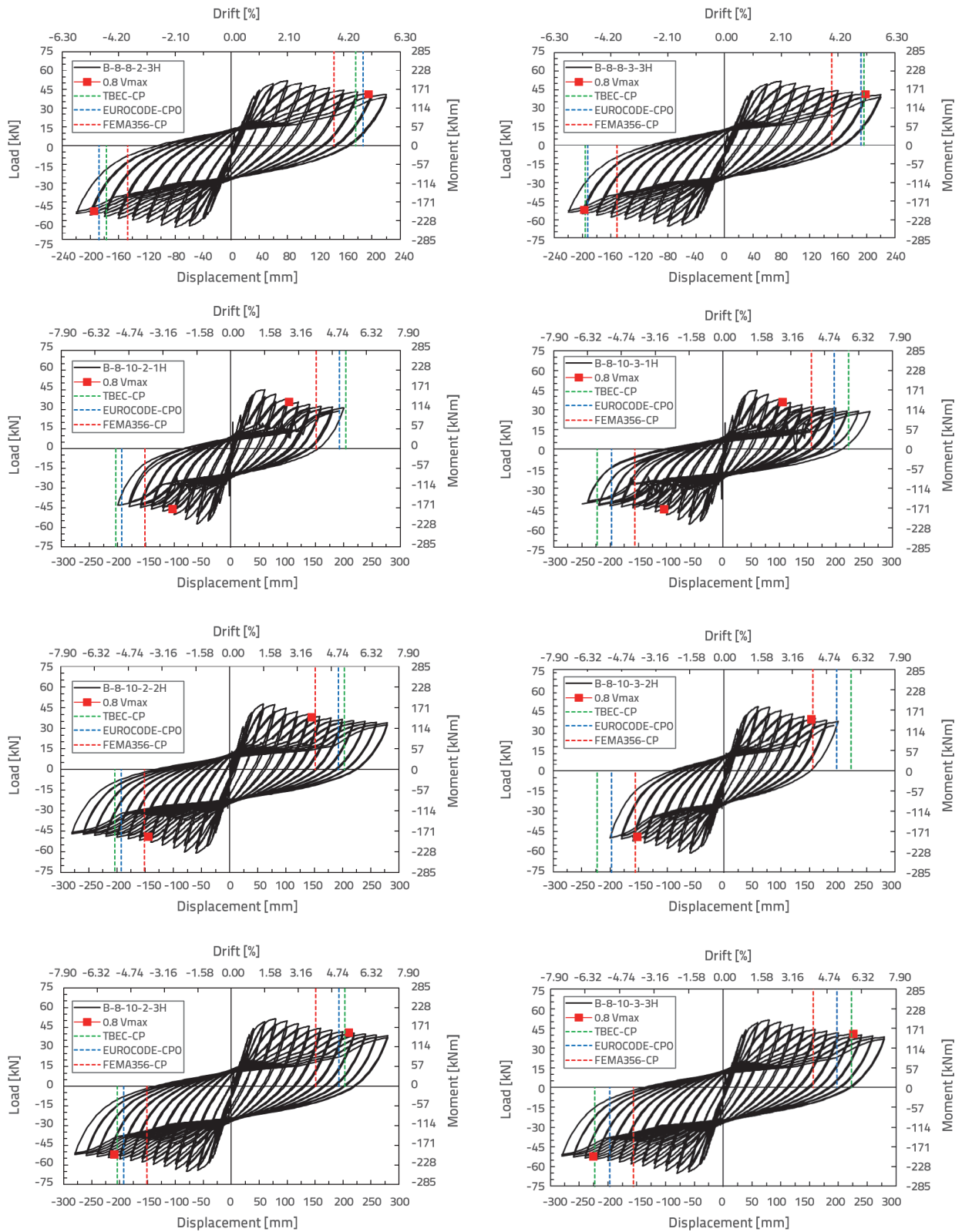


Figure 8. Load–displacement relationships of the beams - continuation 2

Examining the results reveals that FEMA356 yields the most conservative results. Previous studies have determined that TBEC-2018 provides more conservative results in columns [27]. In contrast, TBEC-2018 stands out as the seismic code with the highest beam capacity estimation.

4.1. Backbone curves

Using the backbone curve, the available ductility of the beam considering its post-failure response to cyclic

loads can be evaluated more precisely. In this study, the backbone curves were obtained according to the FEMA356 code.

Figure 9 depicts the schematic backbone curve and sample beams backbone curve. The backbone curves have been combined on the same graphs to compare the results of all beams examined within the scope of the study.

The combined backbone curves prepared in this context are shown in Figure 10.

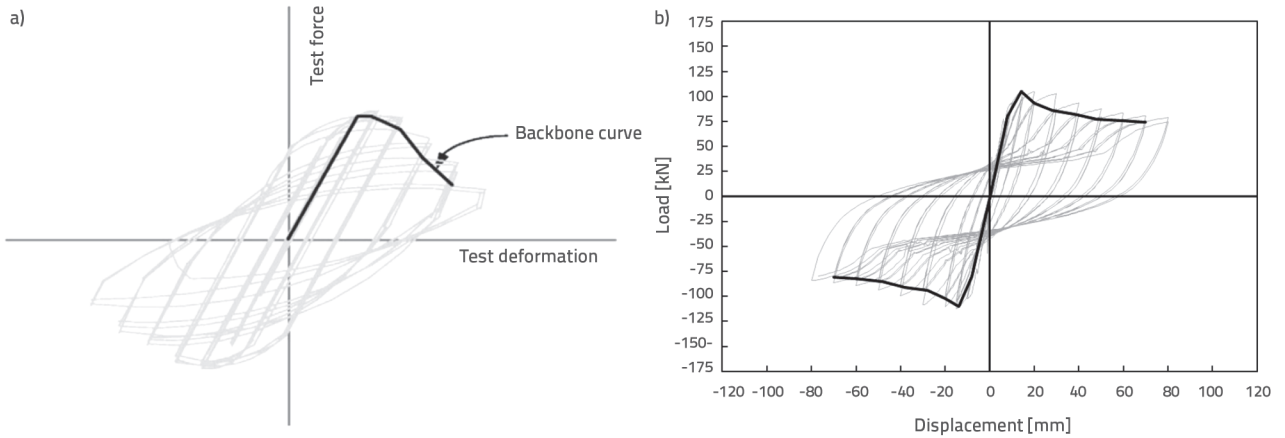


Figure 9. a) Typical cyclic curve and its corresponding backbone curve; b) backbone curve of B-4-8-2-1H

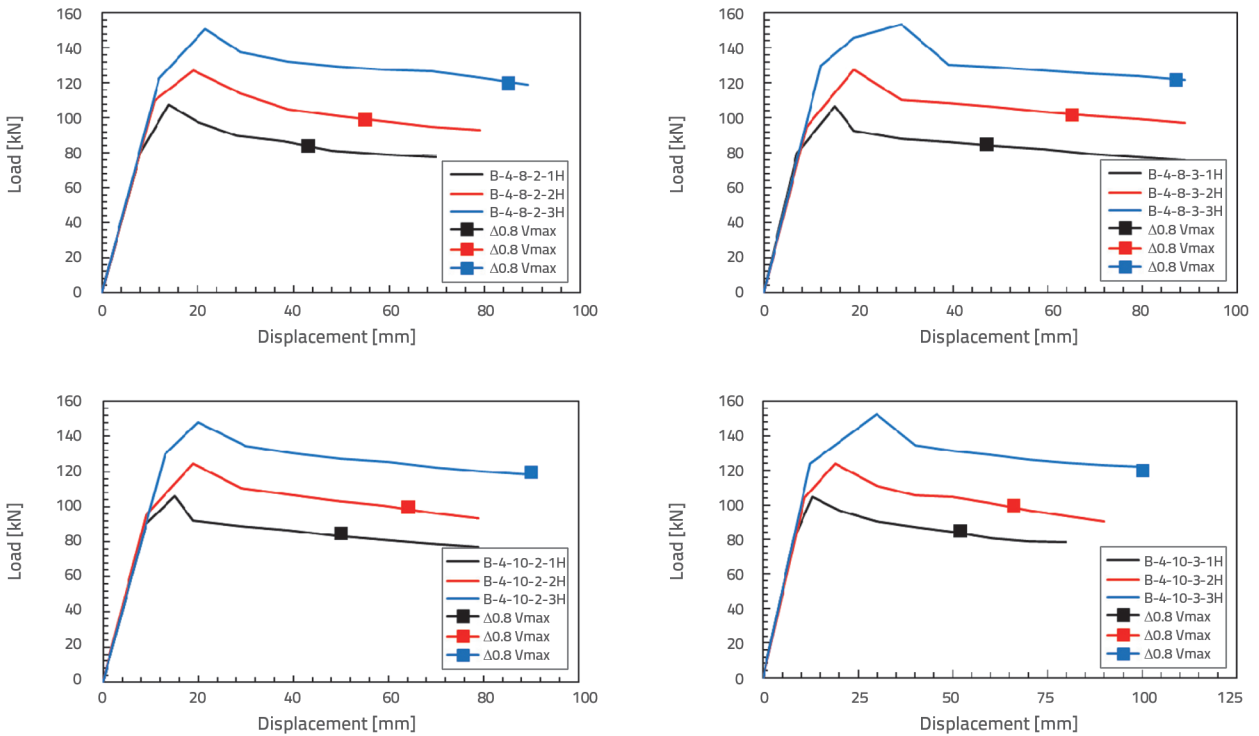


Figure 10. Backbone curves of the beams

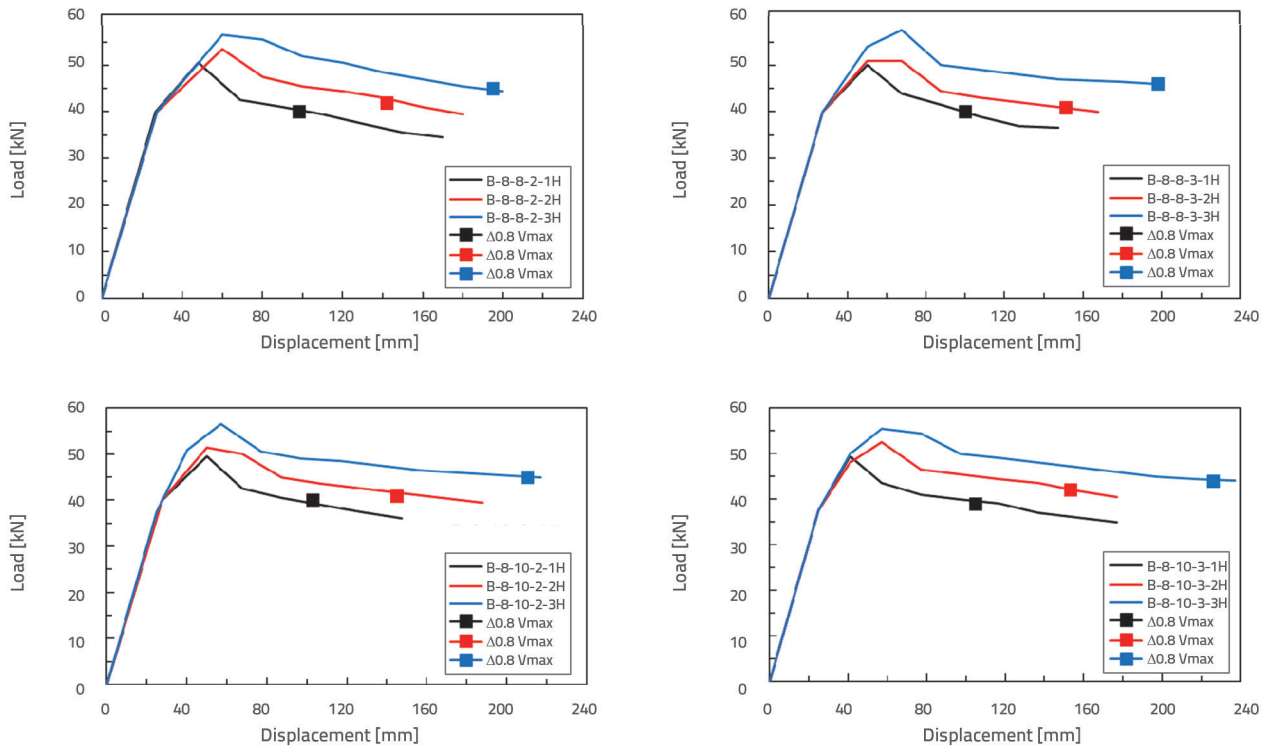


Figure 10. Backbone curves of the beams - continuation

5. Proposed model for tightening zone length

Analytical models have revealed a correlation between the length of the tightening zone and the shear span ratio. In this context, the length of the tightening zone should be expressed as a function of the shear span ratio. The proposed formula is shown in Equation 9.

$$L_{cr} = 1,7 + 0,16 (a/d) \tag{9}$$

where L_{cr} is the beam tightening zone length. Five analytical models with varying shear spans were developed to verify the proposed equation. The properties of confirmation beams with varying shear spans are shown in Table 2.

The analytical results of the confirmation models are shown in Figure 11.

Based on the results, the length of the tightening zone calculated according to the proposed equation yields results consistent with all seismic codes. In addition, the displacement capacities calculated according to all seismic codes for the proposed tightening zone length remained within the safe zone.

Table 2. Properties of confirmation beams with different shear spans

Beam	a/d	ϕ_s	s	Tightening zone	Shape of stirrup
B-2	2	8	$\emptyset 8/7.5/15$	2.00 h	2
B-4	4	8	$\emptyset 8/7.5/15$	2.35 h	2
B-6	6	8	$\emptyset 8/7.5/15$	2.65 h	2
B-8	8	8	$\emptyset 8/7.5/15$	2.95 h	2
B-10	10	8	$\emptyset 8/7.5/15$	3.30 h	2

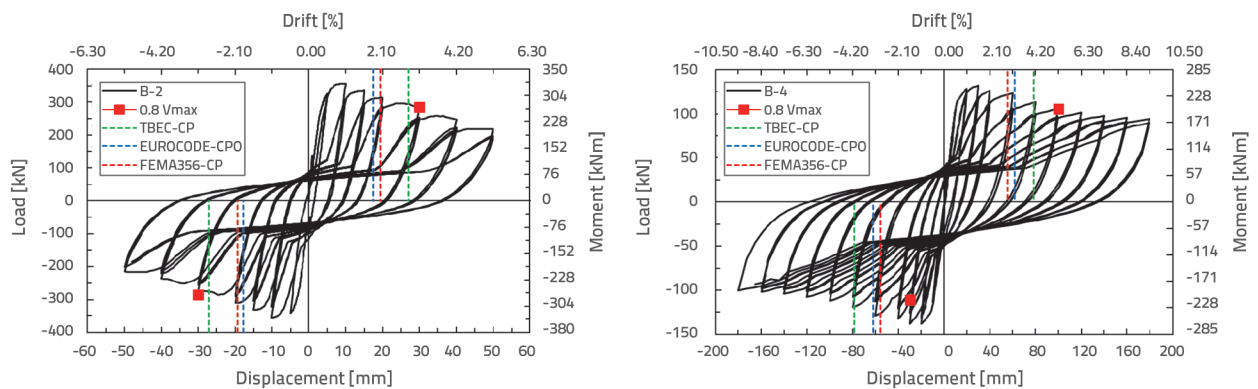


Figure 11. Load–displacement relationships of the confirmation beams

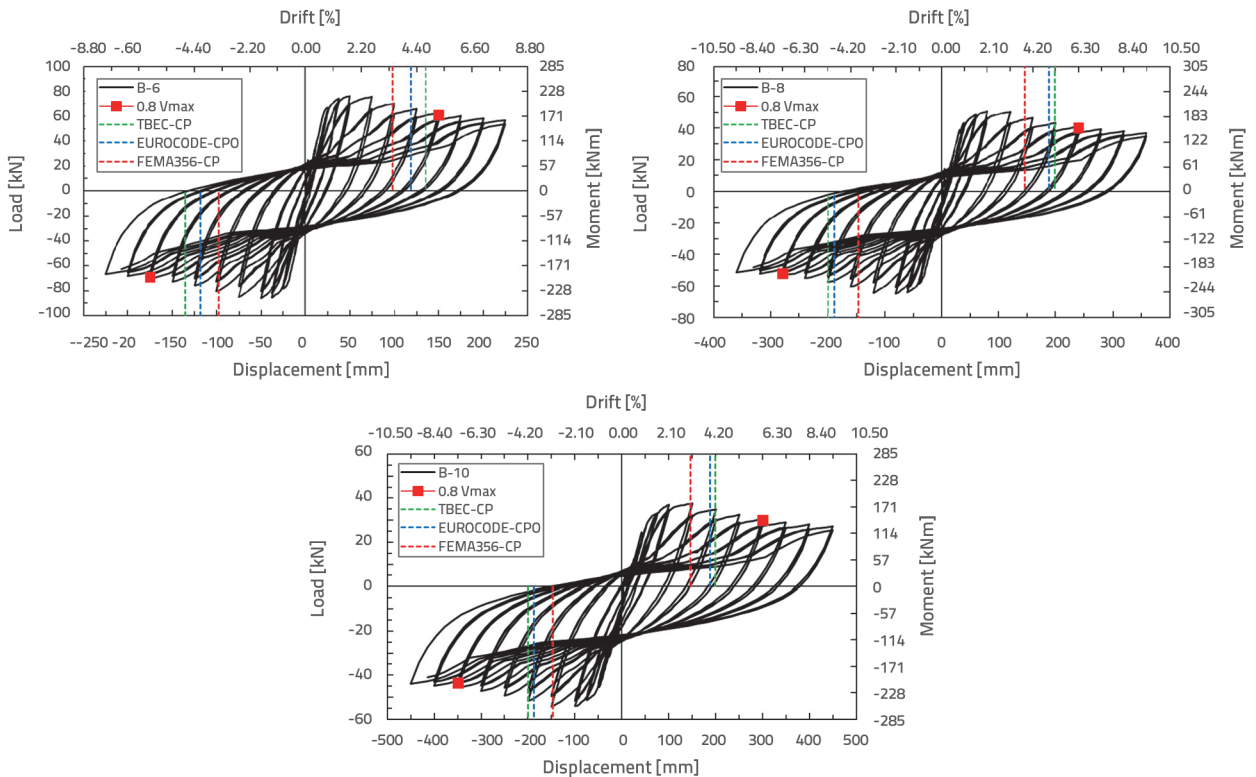


Figure 11. Load–displacement relationships of the confirmation beams - continuation

6. Conclusion

This study investigated the effect of the length of the tightening zone on the beam capacity. The results of the study are listed as follows:

- As the length of the tightening zone increases (especially 3h), the displacement capacity also increases. However, the increase in lateral load capacity is more limited.
- Considering the lateral load and displacement capacity, the influence of the diameter and shape of the stirrup is minimal. As the length of the tightening zone increases for beams with a 10 mm stirrup diameter, the lateral load capacity increases significantly. Therefore, the increase in stirrup diameter and length of the tightening zone contributes significantly to the beam capacity.

- The highest and lowest displacement capacity estimate for all beams was made by TBEC-2018 and FEMA356, respectively.
- In all seismic codes, when the length of the tightening zone is 2h, the displacement capacity of beams with a high shear span ratio is calculated to be higher than the true value. In beams with a tightening zone length of 3h, all seismic codes produce results closer to the actual displacement capacity.
- According to the results of the limited number of analytical models, it would be preferable to increase the tightening zone length to 3h, particularly in beams with high shear spans.
- It was observed that the proposed equation within the scope of the study yields safe results for all seismic codes. In this context, it is believed that all seismic codes would be more accurate in expressing the length of the tightening zone depending on the shear opening.

REFERENCES

- [1] Kwak, H. G., Kim, S.P.: Nonlinear analysis of RC beams based on moment-curvature relation. *Computers & Structures*, 80 (2002) 7-8, pp. 615–628.
- [2] Demir, A., Ince, Y., Altioek, T.Y.: Experimental and numerical investigation of RC beams strengthened with CFRP composites, *Građevinar*, 73 (2021) 6, pp. 605–616, <https://doi.org/10.14256/JCE.3051.2020>.
- [3] Ninčević, K., Ožbolt, J., Boko, I.: The influence of continuing reinforcement on the load capacity of a RC beam previously exposed to high temperatures, *Građevinar*, 68 (2016) 12, pp. 967–978, <https://doi.org/10.14256/JCE.1667.2016>
- [4] Stochino, F.: RC beams under blast load: Reliability and sensitivity analysis. *Engineering Failure Analysis*, 66 (2016), pp. 544–565.
- [5] Vegera, P., Vashkevych, R., Blikharsky, Z.: Fracture toughness of RC beams with different shear span. In *MATEC Web of Conferences*, 174 (2018), pp. 02021, EDP Sciences.
- [6] Štimac, I., Kožar, I., Mihanović, A.: Beam damage detection by deflection influence lines, *Građevinar*, 59 (2007) 12, pp. 1053–1066.
- [7] Yu, Q., Bažant, Z.P.: Can stirrups suppress size effect on shear strength of RC beams? *Journal of Structural Engineering*, 137 (2011) 5, pp. 607–617.

- [8] Russo, G., Mitri, D., Pauletta, M.: Shear strength design formula for RC beams with stirrups. *Engineering Structures*, 51 (2013), pp. 226–235.
- [9] Hu, B., Wu, Y.F.: Effect of shear span-to-depth ratio on shear strength components of RC beams. *Engineering Structures*, 168 (2018), pp. 77–783.
- [10] Al-Sheikh, S.A.: Flexural behavior of RC beams with opening. *Concrete Research Letters*, 5 (2014) 2, pp. 812–824.
- [11] Allam, S.M.: Strengthening of RC beams with large openings in the shear zone. *Alexandria Engineering Journal*, 44 (2005) 1, pp. 59–78.
- [12] Ou, Y.C., Nguyen, N.D.: Plastic hinge length of corroded reinforced concrete beams. *ACI Structural Journal*, 111 (2014) 5, pp. 1049.
- [13] Zhao, X., Wu, Y.F., Leung, A.Y., Lam, H.F.: Plastic hinge length in reinforced concrete flexural members. *Procedia Engineering*, 14 (2011), pp. 1266–1274.
- [14] Cansız, S.: Analytical Estimation of the Residual Drift of Reinforced Concrete Columns under the Ultimate Displacement Capacity. *Periodica Polytechnica Civil Engineering*, 65 (2021) 2, pp. 450–462.
- [15] Ali, U., Ahmad, N., Mahmood, Y., Mustafa, H., Munir, M.A.: A comparison of Seismic Behavior of Reinforced Concrete Special Moment Resisting Beam-Column Joints vs. Weak Beam Column Joints Using Seismostruct. *J. Mech. Contin. Math. Sci*, 14 (2019) 3, pp. 289–314.
- [16] Saeed, H.Z., Ahmed, A., Ali, S.M., Iqbal, M.: Experimental and finite element investigation of strengthened LSC bridge piers under Quasi-Static Cyclic Load Test. *Composite Structures*, 131 (2015), pp. 556–564.
- [17] CEN, "Eurocode 8: Design of structures for earthquake resistant, Part 1", Comité Européen de Normalisation, Brussels, 2003.
- [18] TBEC (2018), Turkey Building Earthquake Code, Specifications for Structures to be Built in Disaster Areas, Ankara. [online] Available at: <https://www.afad.gov.tr/turkiye-bina-deprem-yonetmeligi>
- [19] Panagiotakos, T.B., Fardis, M.N.: Deformation of reinforced concrete members at yielding and ultimate, *ACI Structural Journal*, 98 (2001) 2, pp. 135–48.
- [20] FEMA-356. Prestandard and commentary for the seismic rehabilitation of buildings. Report No. FEMA-356, Federal Emergency Management Agency, Washington, D.C., 2000. [online] Available at: https://www.fema.gov/media-library-data/20130726-1444-20490-5925/fema_356.pdf
- [21] A computer program for static and dynamic nonlinear analysis of framed structures. 2020. [online] Available at: <http://www.seissoft.com>.
- [22] Aydemir, C., Eser Aydemir, M., Yıldırım, P.: Belirgin Düşey Yük Etkisindeki Betonarme Kirişlerin Çevrimsel Yükler Altındaki Davranışı Üzerine Deneysel Bir İnceleme. *Teknik Dergi*, 2020, <https://doi.org/10.18400/tekderg.34140>.
- [23] Lehman, D.E., Moehle, J.P.: Seismic performance of well-confined concrete bridge columns. PEER-1998/01. Pacific Earthquake Engineering Research Center, University of California, Berkeley, 2020.
- [24] Sashi, K.K., Ashraf, E.B., Andrew, W.T., Pinto P.E.: Method of analysis for cyclically loaded R.C. plane frames including changes in geometry and non-elastic behaviour of elements under combined normal force and bending. Symposium on the Resistance and Ultimate Deformability of Structures Acted on by Well Defined Repeated Loads, International Association for Bridge and Structural Engineering, Zurich, Switzerland, (1973), pp. 15–22.
- [25] Mander, J.B., Priestley, M.J.N., Park, R.: Theoretical stress-strain model for confined concrete. *Journal of Structural Engineering*, 114 (1988) 8, pp. 804–1826.
- [26] Cansız, S., Aydemir, C., Arslan, G.: Comparison of displacement capacity of reinforced concrete columns with seismic codes. *Advances in concrete construction*, 8 (2019) 4, pp. 295–304.